Probabilistic sensitivity of base-isolated buildings to uncertainties

Hatice Gazi[a] and Cenk Alhan[*]

Department of Civil Engineering, İstanbul University - Cerrahpaşa, Avcılar Campus, Avcılar, İstanbul, Turkey

Abstract.　Characteristic parameter values of seismic isolators deviate from their nominal design values due to uncertainties and/or errors in their material properties and element dimensions, etc. Deviations may increase over service life due to environmental effects and service conditions. For accurate evaluation of the seismic safety level, all such effects, which would result in deviations in the structural response, need to be taken into account. In this study, the sensitivity of the probability of failure of the structures equipped with nonlinear base isolation systems to the uncertainties in various isolation system characteristic parameters is investigated in terms of various isolation system and superstructure response parameters in the context of a realistic three-dimensional base-isolated building model via Monte Carlo Simulations. The inherent record-to-record variability nature of the earthquake ground motions is also taken into account by carrying out analyses for a large number of ground motion records which are classified as those with and without forward-directivity effects. Two levels of nominal isolation periods each with three different levels of uncertainty are considered. Comparative plots of cumulative distribution functions and related statistical evaluation presented here portray the potential extent of the deviation of the structural response parameters resulting from the uncertainties and the uncertainty levels considered, which is expected to be useful for practicing engineers in evaluating isolator test results for their projects.

Keywords:　probabilistic analysis; sensitivity analysis; Monte Carlo simulation method; uncertainty; seismic performance; base isolation

1. Introduction

Mechanical characteristics governing force-displacement relationships of seismic isolators vary over service life of isolators and deviate from their nominal values determined via the prototype tests as a result of environmental effects and service conditions (Cheng *et al*. 2008). For accurate analysis and design of seismically isolated structures, such effects causing variabilities or deviations in mechanical properties of isolation elements and consequently in structural response parameters from their nominal design values should be taken into account (ASCE/SEI 7-10). In current design practice, these random effects are being taken into account via the property modification coefficients (Constantinou *et al*. 1999) which are applied to the mechanical properties of isolators in the context of a deterministic approach. There are also important additional factors causing variabilities or deviations in the mechanical parameters of the seismic isolators and consequently in the structural response such as uncertainties and/or errors in their material properties, element dimensions, etc. (De La Llera 1994, Shenton III and Holloway 2000). Moreover, the earthquake excitations are inherently random (Jangid and Datta 1995a) due to uncertainties that exist in the active faults and the local soil conditions (Datta 2010) and thus show record-to-record

variability.

Most previous studies related to seismically isolated buildings consider mechanical characteristics of the isolation systems as deterministic parameters and make use of a small number of earthquake ground motions or ground motion spectra, which can't adequately represent the inherent uncertainty of the problem that is defined above. Among them, Yoo and Kim (2002), Alhan and Gavin (2004), Providakis (2009), Mazza *et al*. (2012), Alhan *et al*. (2016) investigated variation of the dynamic responses of the structural systems under selected ground motion records via deterministic parametric analyses while other researchers concentrated on the eccentricities that occur due to various distributions of seismic isolators in plan with different mechanical characteristics (Matsagar and Jangid 2005, Tena-Colunga and Zambrana-Rojas 2006, Kilar and Koren 2009). There are also studies that make use of a large number of deterministic values for characteristic parameters of isolation system and/or ground motions in order to investigate the deterministic sensitivity of the structural response parameters to variations in the aforementioned parameters (Su *et al*. 1990a, Fan *et al*. 1991). In a comprehensive deterministic sensitivity study, Alhan and Hışman (2016) investigated the sensitivity of base displacements and top floor accelerations of a multi-story shear building frame to pre-determined constant deviations in superstructure and isolation system characteristic parameters such as yield strength, yield displacement, and stiffness ratio from the nominal design values. Likewise, Choun *et al*. (2014) conducted deterministic seismic response analyses for a nuclear island, with or without eccentricity in the isolation system due to stiffness variation

∗Corresponding author, Professor
　E-mail: cenkalhan@istanbul.edu.tr
[a] Ph.D.
　E-mail: hgazi@istanbul.edu.tr

of ±20% assumed to be identical for each individual isolator and investigated the effects of the subject variation on the seismic response.

There also exist studies which investigate dynamic response of seismically isolated structures via probabilistic analyses most of which use a random earthquake excitation model but the mechanical characteristics of the isolation system parameters are rather varied parametrically in the context of a deterministic approach in order to investigate their effects on the structural response. For example, Jangid and Datta (1995b) studied the sensitivity of stochastic response of an asymmetric building equipped with various isolation systems to the parametric variations in the structural parameters related to the superstructure and isolator eccentricities. In another study, Marano and Greco (2003) investigated the sensitivity of the seismic response parameters of a generic shear-type building isolated by high damping rubber bearings (HDRBs) to parametric variations related to the isolation system characteristics. Recently, Jangid (2010), Ma *et al.* (2011), Jacob *et al.* (2013), and Ma *et al.* (2014) carried out stochastic response analyses for seismically isolated structures under random earthquake excitations and investigated the effects of deterministic variations in the isolation system and/or other structural system characteristics on the dynamic response of those structures.

There are other studies which take the uncertainties existing in the characteristic properties of seismic isolators into account by modeling some of these properties as random some of which use random earthquake models while others use a few historical earthquake records. Among them, Hirata *et al.* (1989) investigated the effect of randomness of pre-yield stiffness of isolators, which are assumed to be normally distributed, on the displacement response and the eccentricity of a rigid base-mat that is modeled as a single degree of freedom system via Monte-Carlo simulations. Pinto and Vanzi (1992) also conducted a sensitivity analysis for the superstructure and base displacements of a two-degree-of-freedom system, which is isolated with HDRBs by assuming the secant stiffness of the isolation system and the elastic stiffness of the superstructure as normally distributed random variables. De La LLera and Inaudi (1994) assumed the lateral stiffness of the linear seismic isolators of an isolation system under a rigid diaphragm as independent log-normal random variables and studied the sensitivity of base displacements to the coefficients of variation of the lateral stiffness via Monte Carlo simulations. Shenton III and Holloway (2000) considered the lateral stiffness of the linear isolators of a structure, modelled as a two degree of freedom system, as normally distributed random variables and investigated the sensitivity of the centerline displacement, rotation, corner displacement and base shear parameters of the subject structure with respect to coefficients of variation of the isolator stiffness, aspect ratio of the structure, and/or the number and layout of isolation bearings via analytical solutions and Monte-Carlo simulations. Politopoulos and Sollogoub (2005) studied the vulnerability of a two-degree-of-freedom system consisting of a linear elastic-perfectly plastic superstructure and an isolation system composed of

isolators whose lateral stiffness are modeled as normally distributed random variables via Monte Carlo simulations. Alhan and Gavin (2005) investigated the sensitivity of reliability of a floor isolation system that is located on a floor of a fixed base building, to the variances in the random stiffness and damping parameters of the linear isolators via Monte Carlo simulations. Okamura and Fujita (2007) investigated the sensitivities of base displacements and accelerations of two structural systems, which are isolated with curved surface sliders, to the friction coefficients of the bearings and the vertical loads on the same bearings via Monte Carlo simulations by assuming aforementioned random parameters as normally distributed. Politopoulos and Pham (2009) investigated the sensitivity of seismically isolated structures to small variabilities in earthquake loading and isolation system and superstructure characteristics via Monte Carlo simulations using two-degree-of-freedom systems which have superstructures with different idealized nonlinear constitutive laws isolated with passive active and semi-active control systems. Having facilitated the nonlinear-force deformation characteristics of the isolators by using the stochastic linearization method, Mishra and Chakraborty (2013) evaluated the sensitivities of the top floor displacements and accelerations of a five-story base-isolated building, which is idealized as a two-dimensional shear frame where the characteristic parameters of the isolators are modeled as normally distributed uncertain random variables. They concluded that the stochastic response of the structural system is affected both by the randomness of the ground motion parameters and by the uncertainty in the system parameters. Fan and Zhang (2014) proposed a method in order to calculate the fragility curves of bearing failure in the isolated structures taking into account the uncertainties in elastic stiffness and damping of the linear rubber-based bearings, friction coefficient and axial force of the friction bearings, mass matrix of the base, stiffness and mass matrices of the superstructure. Han *et al.* (2014) conducted seismic risk analyses for a typical mid-rise reinforced concrete frame building before and after retrofitting with base isolation considering uncertainties in the parameters of the structural system and the isolation system, and using a suite of recorded mainshock and aftershock ground motions. In addition, Castaldo and his friends conducted a series of studies related to the reliability of seismically isolated buildings equipped with friction pendulum systems, taking into account the uncertainties in both the parameters of the isolation system and the ground motion excitations. In a current study, Castaldo *et al.* (2017) investigated the seismic reliability of a two-degree-of-freedom building isolated by frictional pendulum system and subjected to artificial ground motions taking into account the friction coefficient of the isolators as uniformly distributed random variable as well as the fundamental circular frequency and damping factor parameters of the soil strata included in the power spectral density function of the ground motion model determined by modified Kanai-Tajimi filter.

It is clearly seen that most previous sensitivity studies related to seismically isolated buildings are deterministic. In the probabilistic ones, the elements of the seismic isolation
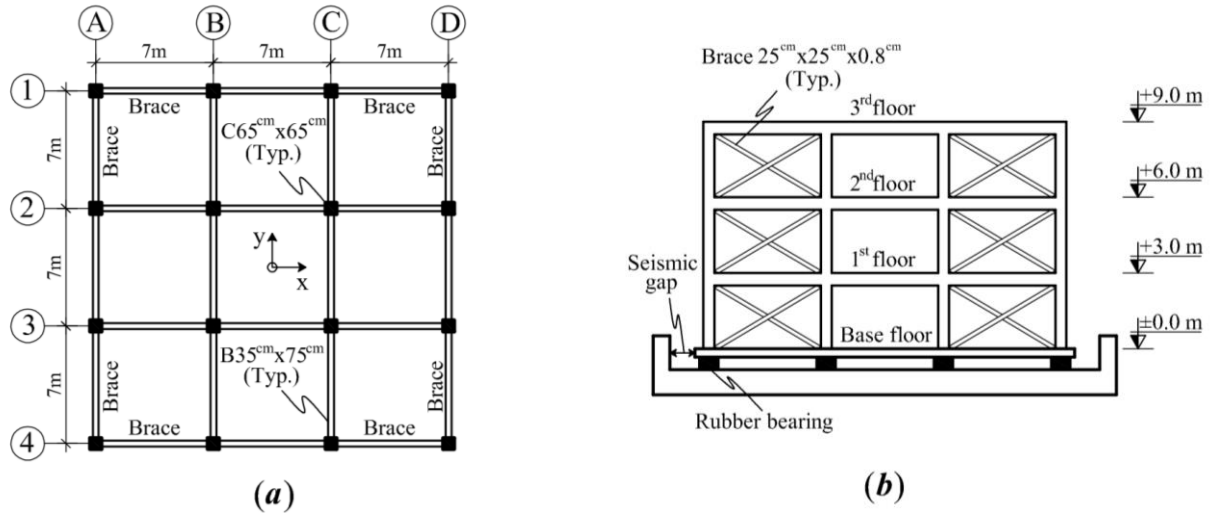
Fig. 1 Typical (a) floor plan and (b) elevation view of the benchmark building

systems are either modeled as linear or equivalent linear counterparts of nonlinear isolation system elements and/or the superstructure is modeled as simple single or few degree-of-freedom systems or idealized two dimensional shear frames. Moreover, the record-to-record variability of ground motions records are not adequately taken into account as a limited number of historical ground motion records are used owing to time consuming nature of such studies. Considering these issues, this study focuses on investigating the sensitivity of the probability of failures of structures equipped with nonlinear isolation systems to the uncertainties in the nonlinear isolator parameters in terms of various isolation system and also superstructure response parameters in the context of a realistic three dimensional multi-story structural model. In particular, the inherent record-to-record variability nature of the problem is taken into account by using a large number of ground motion records which are further classified as those with and without forward-directivity effects. Two different levels of isolation periods, each with three different levels of uncertainty, are considered. Pre-yield stiffness, post-yield stiffness, and yield displacement characteristics of each isolator are assumed as random variables. Biaxial interaction between the isolators are also taken into account in the bidirectional nonlinear time history analyses carried out in the framework of Monte Carlo Simulations.

2. Structural model

In this study, a realistic base-isolated building with four floors (including the base) is considered as the benchmark building (see Fig. 1). The base floor is supported by an isolation system consisting of 16 rubber-based isolators each of which is placed underneath each column. The overall geometry, the geometrical properties of the structural elements and the associated material properties of the superstructure are obtained from Tena - Colunga and Escamilla - Cruz (2007). Although the isolation system

layout is identical to Tena - Colunga and Escamilla - Cruz (2007), the specific properties of the isolators, which are taken as random in this study, are completely different as explained below.

The superstructure is composed of A36 steel braces and reinforced concrete ($f_c \approx 25$ N/mm^2, $E_c \approx 21708$ N/mm^2) moment resisting frame elements. All floor slabs are modeled as rigid-diaphragms with three degrees of freedom (two translational and one rotational component). Each floor -including the base floor- has a translational mass of 330 kNs^2/m in x and y axes and a rotational mass of 24280 kNs^{2}m about the z axis, which are assumed to be lumped at the center of mass of each floor. The translational fixed-base periods corresponding to the first two modes are equal to 0.18 s, which are the same as those reported in Tena - Colunga and Escamilla - Cruz (2007).

The seismic isolators exhibit nonlinear material behavior and hysteretic energy dissipation under earthquake loading whose force-displacement relationships are modeled as smooth bi-linear hysteretic as shown schematically in Fig. 2. In this figure, K_1, K_2, F_y, Q, and D_y represent the pre-yield stiffness, the post-yield stiffness, the yield force, the characteristic force, and the yield displacement of a typical isolator, respectively.

The nominal values of the aforementioned parameters and the post-yield to pre-yield stiffness ratio parameter ($\alpha = K_2/K_1$) for two main isolation systems (long and short period) considered in this study are listed in Table 1. The relationship between the rigid-body mode periods (T_0) and the post-yield stiffness (K_2) of the isolators is given in Eq. (1). In this equation, M is the total translational mass of the base-isolated building, which is equal to 1320 kNs^2/m, while n_b represents the total number of isolators in the isolation system.

$$K_2 = \left(4\pi^2 M\right)/\left(n_b T_0^2\right) \tag{1}$$

The characteristic force of an isolator (Q), which is the shear force at zero displacement for a hysteresis loop, is generally used for estimating the stability of hysteretic behavior when the isolator is exposed to many loading cycles (Cheng *et al.* 2008).
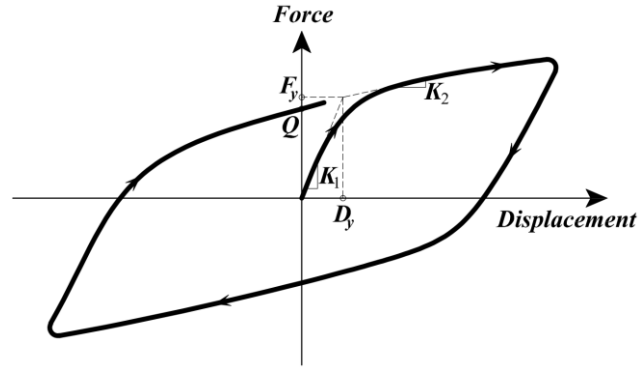
Fig. 2 Force-displacement relationship of the isolators

Table 1 Nominal values of the characteristic isolator parameters

Isolator Characteristic Parameter	Benchmark Isolation System	
	Short-period ($T_0 = 2.0$ s)	Long-period ($T_0 = 3.5$ s)
K_1 (kN/m)	8150.650	2661.440
K_2 (kN/m)	815.065	266.144
D_y (mm)	5.522	16.911
F_y (kN)	45.008	45.008
Q (kN)	40.507	40.507
α (-)	0.100	0.100

As reported by Kelly (2001) the characteristic strength ratio (Q/W) usually ranges from 3% in the regions with low seismicity to 10% in the regions with high seismicity. There are many research studies (Ryan and Chopra 2004, Sharma and Jangid 2009, Ryan and Earl 2010, Kumar 2015) considering values for Q/W in this range. Compatible with this range, the nominal value of the characteristic strength ratio (Q/W) for the isolators is assumed as 5% here. In this study, the yield displacements of the isolators in the benchmark isolation systems are defined using Eq. (2) (Naeim and Kelly 1999) since the parameters Q, K_1 and K_2 are determined as described above. The values considered for D_y here fall within the typical range reported in the seismic isolator manufacturers catalogues (DIS, 2007). Finally, the yield force (F_y) of the isolators, corresponding to the values of D_y, is defined by Eq. (3) (Naeim and Kelly 1999) which is obtained from the initial elastic part (K_1) of the force-displacement relationship curve of the isolators seen in Fig. 2.

$$D_y = Q/(K_1 - K_2) \qquad (2)$$

$$F_y = K_1 \times D_y \qquad (3)$$

3. Probabilistic model of the benchmark isolation systems

In the context of the Monte Carlo Simulation Method, which is employed in this study, the characteristic parameters of the benchmark isolation system elements are modeled as random variables. Three different levels of uncertainty, namely 5%, 10%, and 15% coefficient of variation (*C.O.V.*) is considered for the random variables, which results in 6 subsets of isolation systems as shown in Table 2. The first three subsets are generated based on the 1st benchmark isolation system, whose nominal period is equal to 2.0 s (labeled as T0nom20) based on nominal isolator characteristic parameters. Likewise, the second three subsets are generated based on the 2nd benchmark isolation system with nominal period of 3.5 s (labeled as T0nom35).

In brief, the following steps are carried out in the scope of the subject Monte Carlo Simulation Technique in order to investigate the probabilistic sensitivity: (i) the problem is defined in terms of all random variables; (ii) the values of the random variables are generated following a specified probabilistic distribution by making use of their mean (nominal) and coefficient of variation values; (iii) the problem is solved for each set of values of the random variables generated in step iii; (iv) probabilistic/statistical information is extracted from the simulated cases (Haldar and Mahadevan 2000). Sample application examples of Monte Carlo Simulation to simple structural elements and systems can be found in Alhan and Gazi (2014).

In this study, K_1, K_2, and D_y are modeled as random variables following a normal distribution using (Haldar and Mahadevan 2000) Eq. (4), where R is the random variable following normal distribution, μ is the mean and σ is the standard deviation of R. In addition, S is a standard normal

Table 2 Evaluated isolation systems employing isolators with random characteristic parameters

Benchmark Isolation System*	Nominal Period T_0 (s)	Subset	*C.O.V.* for random isolator parameters (%)
1	2.0 s	T0nom20C05	5
		T0nom20C10	10
		T0nom20C15	15
2	3.5 s	T0nom35C05	5
		T0nom35C10	10
		T0nom35C15	15

*See Table 1 for nominal values of the characteristic parameters of the associated isolators

variable with zero mean and unit standard deviation, which is obtained from Eq. (5), where U represents uniformly distributed random numbers between 0.0 and 1.0. In order to obtain the values of a random variable (R) using Eq. (4), uniformly distributed random numbers (U) are generated primarily. Then, the subject numbers are transformed to standard normal numbers (S) via F_x^{-1}, which is the inverse function of the cumulative distribution function (F_x) that gives the probability of a random variable attaining a value less than a specified limit value. The standard deviation (σ) of the random variable R is calculated using Eq. (6), where, *C.O.V.* is the coefficient of variation of R. In this study, the mean values (μ) of the random variables (K_1, K_2, and D_y) are equal to nominal values given in Table 1 for each reference benchmark isolation system. The *C.O.V.* values of 5%, 10%, and 15% are used for these random variables in the relevant subset of isolation systems given in Table 2. The other isolator characteristic parameters (α, F_y, and Q) are generated to follow relationships given in Eqs. (2) and (3). It should be noted here that each isolator composing an isolation system are modeled to bear its own independent random characteristic value in each cycle of the Monte Carlo Simulation. The probability density function (PDF) plot of the values of a representative random variable (K_1) generated for a representative isolator (A4) in a representative subset of generated isolation systems (T0nom20C05) is presented in Fig. 3.

$$R = \mu + \sigma \times S \qquad (4)$$

$$S = F_x^{-1}(U) \qquad (5)$$

$$\sigma = C.O.V. \times \mu \qquad (6)$$

The area under the probability density function between two limits gives the probability of a random variable having a value between those two limits while the x axis of the relevant PDF plot represents the generated values of that random variable (Haldar and Mahadevan 2000). As seen in Fig. 3, K_1 data generated for use in the Monte Carlo Simulations fit perfectly to the dashed line representing the normal distribution.
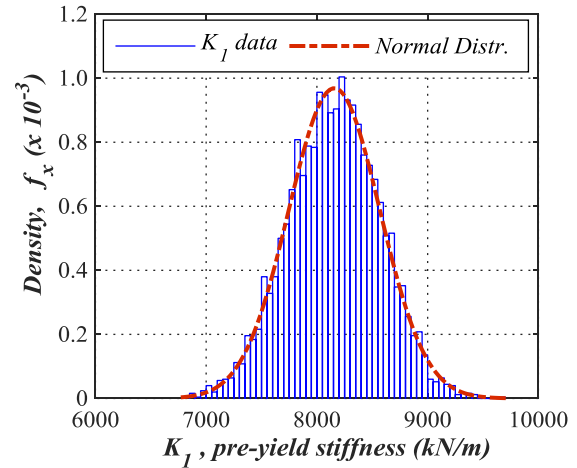

Fig. 3 The Probability Density Plot of K_1 data of the isolator A4 for subset isolation system T0nom20C05

The probability density function plots for all isolator characteristic parameters (K_1, K_2, D_y, α, F_y, and Q) are given in Fig. 4 for the representative A4 isolator for subsets of T_0=3.5 s isolation systems (i.e., for T0nom35C05, T0nom35C10, and T0nom35C15). It should be noted that the number of values generated for each parameter presented here is 5000, which is the number of simulations used in Monte Carlo analysis in this study. The verification of the adequacy of this number is presented in Section 5.2.

4. Earthquake data

In order to take the record-to-record variability into account and obtain a statistically sufficient assessment for the probabilistic sensitivity study carried out here, 108 ground motion records with or without forward directivity effects from 6 historical earthquakes with moment magnitudes varying between 6.7 and 7.6 (the 1999 Chi-Chi Earthquake, the 1999 Kocaeli Earthquake, the 1999 Düzce Earthquake, the 1989 Loma Prieta Earthquake, the 1994 Northridge Earthquake, and the 1992 Erzincan Earthquake) are used. The ground motions with forward directivity effects often have long period velocity pulses with large amplitudes and permanent ground displacements (Somerville 2005, Dicleli and Buddaram 2007). In addition,
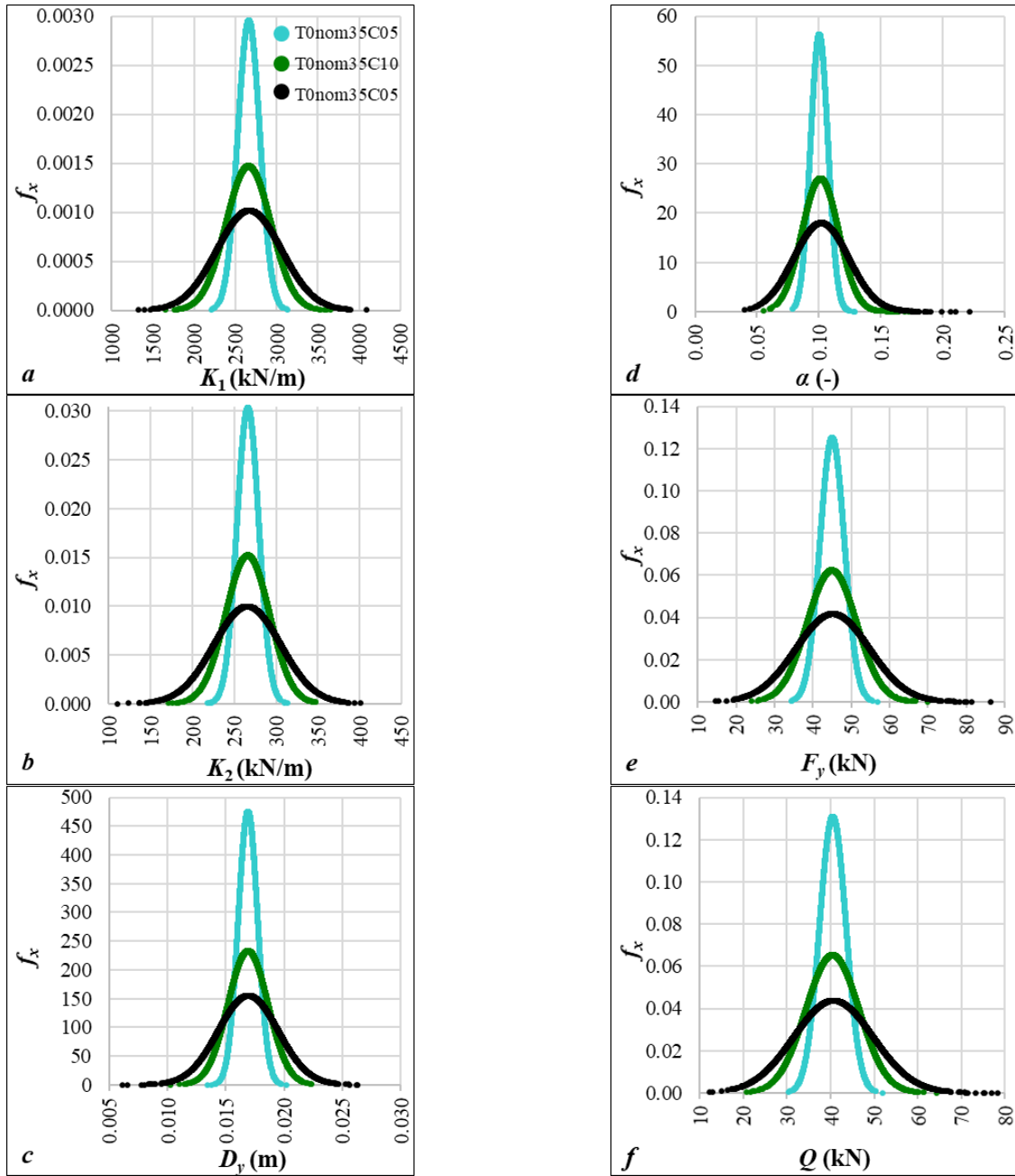
Fig. 4 Probability Distribution Function (PDF) plots of characteristic isolator parameters for the representative case of isolator A4

the subject ground motions generally have higher PGV/PGA ratios and may cause higher seismic responses (particularly in seismically isolated structures) than those, which do not contain directivity pulses but have the same PGA values and duration of shaking (Malhotra 1999). Therefore, in order to reveal the differences in structural system response parameters, the ground motions applied to the buildings in the x direction are grouped into two main categories: 27 of them have forward-directivity effects and listed with FDi codes (i=1-27) on the left side of the table, while the rest 27 do not have forward-directivity effects and listed with NFDi codes (i=1-27) on the right side of Table 3. Results of the bidirectional analyses in the x direction is

presented here. Thus, 54 record components which are applied to the buildings in the x direction are listed in Table 3.

The list of ground motion components given in Table 3 has been obtained from Sehhati *et al.* (2011), who selected those components from a database by Bray and Rodriguez-Marek (2004). The actual records are downloaded from the database of Pacific Earthquake Engineering Research Center (PEER, 2011). The peak ground acceleration (PGA) values and the 10% damped spectral acceleration plots are given in Figs. 5 and 6, respectively.

Table 3 Ground motion components applied in the x direction (adapted from Sehhati *et al.* 2011)

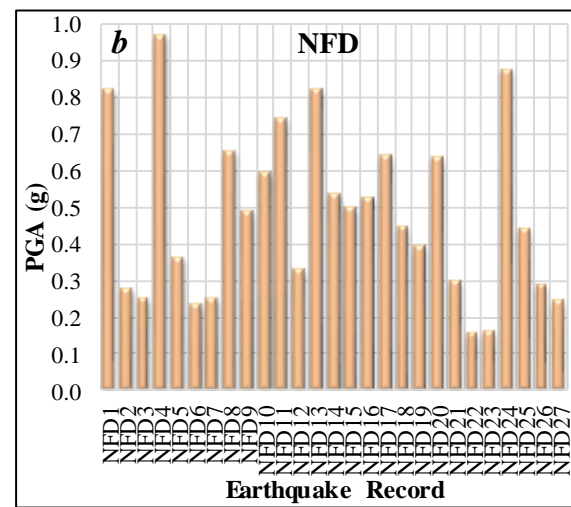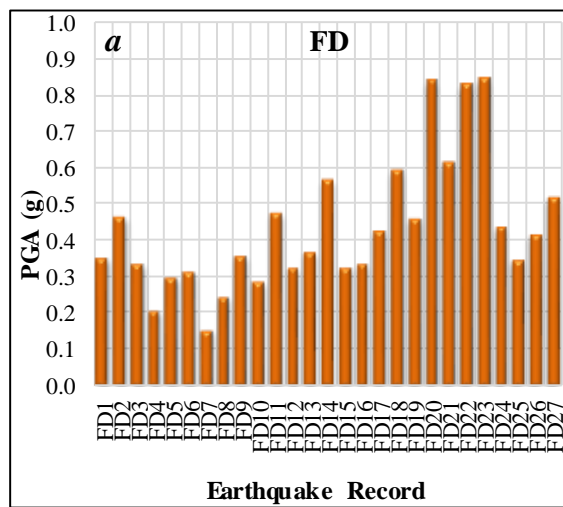| Code	Earth-quake	Station	Component	Code	Earth-quake	Station	Component
FD1	Chi-Chi	TCU052	TCU052-W	NFD1	Chi-Chi	CHY028	CHY028-N
FD2	Chi-Chi	TCU068	TCU068-N	NFD2	Chi-Chi	CHY029	CHY029-W
FD3	Chi-Chi	TCU075	TCU075-W	NFD3	Chi-Chi	CHY035	CHY035-W
FD4	Chi-Chi	TCU101	TCU101-W	NFD4	Chi-Chi	CHY080	CHY080-W
FD5	Chi-Chi	TCU102	TCU102-W	NFD5	Chi-Chi	CHY006	CHY006-E
FD6	Kocaeli	Düzce	DZC-180	NFD6	Chi-Chi	TCU055	TCU055-W
FD7	Kocaeli	Arçelik-	ARC-090	NFD7	Chi-Chi	TCU070	TCU070-W
FD8	Kocaeli	Gebze	GBZ-000	NFD8	Chi-Chi	TCU071	TCU071-N
FD9	Loma P.	Gilroy-	GIL-067	NFD9	Chi-Chi	TCU072	TCU072-W
FD10	Loma P.	Gilroy-	GOF-090	NFD10	Chi-Chi	TCU074	TCU074-W
FD11	Loma P.	Gilroy	GO1-090	NFD11	Chi-Chi	TCU079	TCU079-W
FD12	Loma P.	Gilroy	GO2-090	NFD12	Chi-Chi	TCU089	TCU089-W
FD13	Loma P.	Gilroy	GO3-090	NFD13	Düzce	Bolu	BOL-090
FD14	Loma P.	LGPC	LGP-000	NFD14	Düzce	Düzce	DZC-270
FD15	Loma P.	Saratoga-	STG-090	NFD15	Loma P.	BRAN	BRN-090
FD16	Loma P.	Saratoga-W	WVC-270	NFD16	Loma P.	Capitola	CAP-000
FD17	Northridge	Jensen Filter	JEN-022	NFD17	Loma P.	Corralitos	CLS-000
FD18	Northridge	Newhall-Fire	NWH-360	NFD18	Loma P.	UCSC Lick Obs.	LOB-000
FD19	Northridge	Newhall-W.	WPI-046	NFD19	Loma P.	UCSC	UC2-090
FD20	Northridge	Rinaldi	RRS-228	NFD20	Loma P.	WAHO	WAH-090
FD21	Northridge	Sylmar-	SCS-052	NFD21	Northridge	N Hollywood-	CWC-180
FD22	Northridge	Sylmar-	SCE-018	NFD22	Northridge	Sunland-Mt	GLE-260
FD23	Northridge	Sylmar-Olive	SYL-360	NFD23	Northridge	Burbank-Howard	HOW-330
FD24	Northridge	Pacoima Kagel	PKC-360	NFD24	Northridge	Simi-Valley-	KAT-000
FD25	Northridge	Arleta-	ARL-090	NFD25	Northridge	Sun Valley-	RO3-090
FD26	Northridge	Pacoima Dam	PAC-175	NFD26	Northridge	Santa Susana	SSU-090
FD27	Erzincan	Erzincan	ERZ-NS	NFD27	Northridge	Big Tujunga,	TUJ-352

Fig. 5 Peak ground accelerations for (a) Forward Directivity (FD) ground motions and (b) Non-Forward Directivity (NFD) ground motions
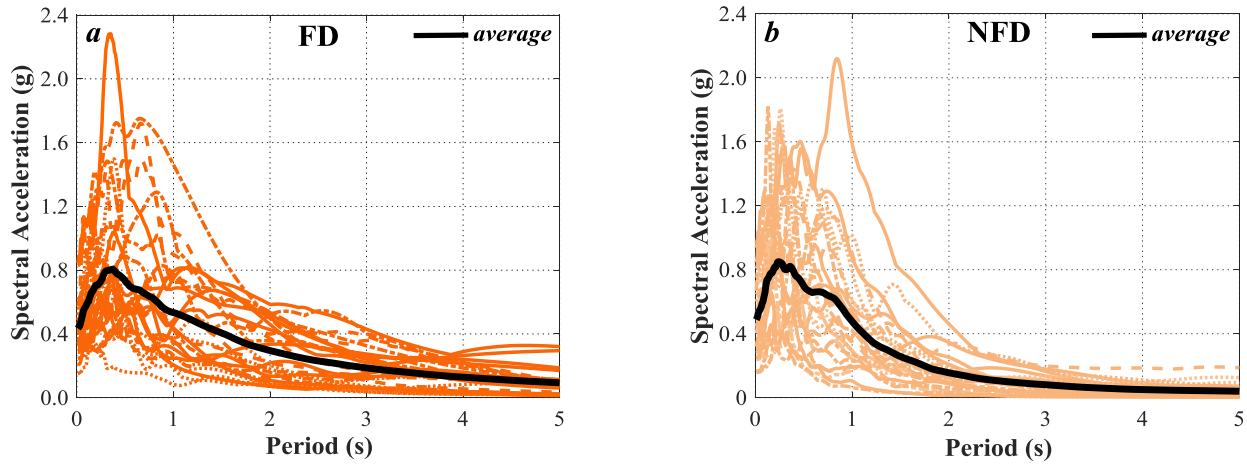
Fig. 6 Spectral accelerations for (a) Forward Directivity (FD) ground motions and (b) Non-Forward Directivity (NFD) ground motions [%10 damped]

5. Sensitivity analyses

In the probabilistic sensitivity analyses, the sensitivity of the probability of failures of (i) peak base displacements (*bdcx*), (ii) peak top floor displacements (*tfdx*), (iii) peak total top floor accelerations (*tfax*), and (iv) peak base shear forces (*bsx*) calculated at the center of mass of the relevant floors to the random deviations in the isolator characteristic parameters from their nominal design values are investigated for different limit states. In order to conduct the required recursive nonlinear time history analyses in the context of the Monte Carlo Simulation, 3D-BASIS-MONTE (Gazi 2015), which is a modified version of 3D-BASIS (Nagarajaiah *et al.* 1991), is used. 3D-BASIS-MONTE (Gazi 2015) accepts input data compatible with the Monte Carlo Simulation method and conducts recursive nonlinear dynamic analyses of base-isolated buildings with different isolation system characteristics subjected to historical earthquakes, while the original version, 3D-BASIS (Nagarajaiah *et al.* 1991), is able to conduct a single run, only. A flowchart for 3D-BASIS-MONTE (Gazi 2015) along with the preparation of random input data and statistical post-processing of the structural response output data in MATLAB (Mathworks 2009) are given in Fig. 7.

For the subject probabilistic sensitivity analysis, cumulative distribution function (CDF) plots of the investigated structural response parameters are obtained for each earthquake at first. In these plots, a normalization is applied in order to present the extent of the deviation of each structural response parameter from its nominal corresponding value (which is obtained by using reference benchmark isolation systems with nominal isolator characteristic parameters) conveniently. That is, the structural response values obtained from Monte Carlo Simulations are divided by the values obtained from nominal reference systems to obtain the aforementioned normalized responses: $bdcx/bdcx_{nom}$, $tfdx/tfdcx_{nom}$, $tfax/tfax_{nom}$, bsx/bsx_{nom}. A sample CDF plot for the normalized peak base displacement response is given in Fig. 8 for T0nom20C05, T0nom20C10, and T0nom20C15

building subsets subjected to FD1. The vertical axes in a typical CDF plot contains information regarding the probability of exceeding a limit state defined in terms of the values in given x-axis. For example, for a limit state of $bdcx/bdcx_{nom}$ =1.05, the probability of $bdcx/bdcx_{nom} \leq$1.05 is equal to 90% (i.e., F_x=0.9) for T0nom20C15 building subset as shown in Fig. 8. Consequently, the probability of exceeding the sample limit state value of $bdcx/bdcx_{nom}$ =1.05 (i.e., the probability of failure, P_f) is equal to 10% (i.e., P_f=1.0-F_x =1.0-0.9=0.1).

For all the response parameters of all the building subsets, CDF curves are obtained for each earthquake loading (similar to the one given in Fig. 8) individually. Then, the average of the CDF values over all earthquakes are calculated for each *C.O.V.* value and presented in a comparative fashion in Figs. 9 and 10. The plots presented in Figs. 9 and 10 include the average CDF values for 27 FD and 27 NFD earthquake loadings, separately. The general observations from these figures can be listed as follows: (1) the levels of sensitivity all of the structural response parameters steadily increase as the *C.O.V.* values of the isolator characteristic parameters increase from 5% to 10%, and 15%. (2) the shapes of CDF plots of displacement related parameters (*bdcx* and *tfdx*) -for a particular building subset and earthquake loading- in general resemble each other. The same is true for acceleration related parameters (*tfax* and *bsx*). (3) the shapes of CDF plots of a particular response parameter of a particular building subset in general resemble each other for different earthquake loading types (FD and NFD) and also for different isolation system types (T0nom20 and T0nom35). The details of these general observations are further assessed in Section 5.1.

The extreme values of the normalized structural responses (those correspond to the highest and lowest F_x values) obtained from CDF plots given in Figs. 9 and 10 are presented in Fig. 11. The observations from these figures are: (1) Regardless of (i) the earthquake type (FD and NFD), (ii) the structural response parameter type, and (iii) the nominal periods of the building subsets, normalized values of structural response parameters averaged over all
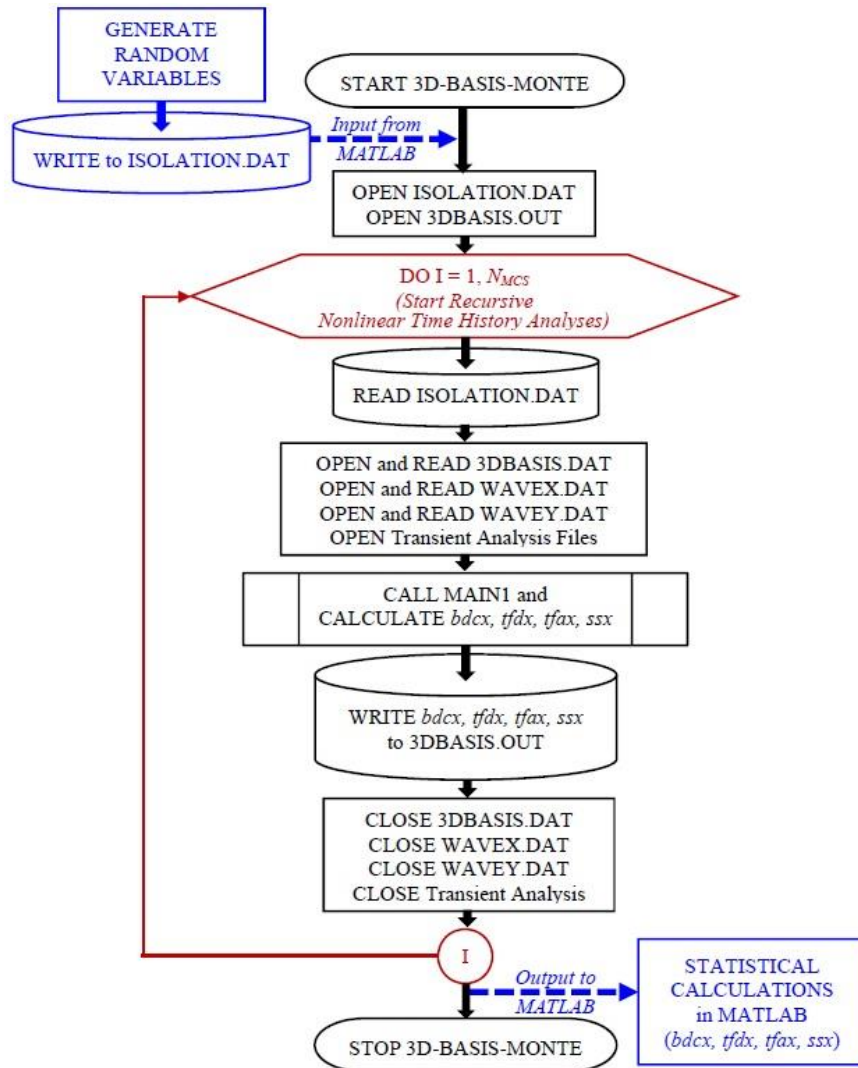
Fig. 7 Outline Flowchart of 3D-BASIS-MONTE (Gazi, 2015) [ISOLATION.DAT contains the isolation system data; 3DBASIS.DAT contains the remaining data related to the structural system; WAVEX.DAT and WAVEY.DAT contain ground motion acceleration data applied to the structural system in the x and y directions, respectively; MAIN1 is the subroutine program conducting all the necessary calculations; N_{MCS} is the Number of Monte of Monte Carlo Simulations]
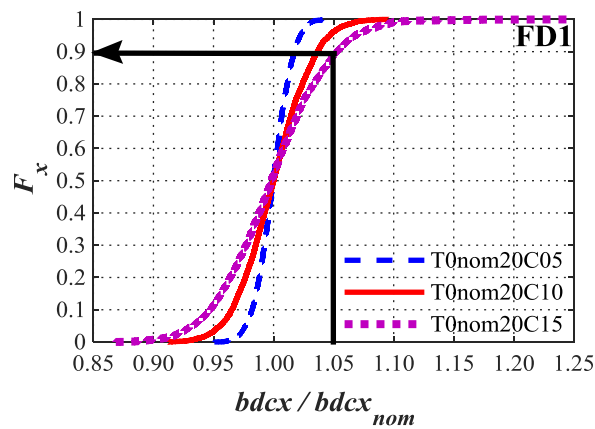

Fig. 8 Cumulative Distribution Function (CDF) plots for normalized peak base displacement -calculated at the center of mass, normalized with respect to corresponding nominal value, and for FD1earthquake. [Arrow shows a sample reading, i.e., probability of exceedance (which is 10%) corresponding to the normalized peak base displacement value of 1.05]
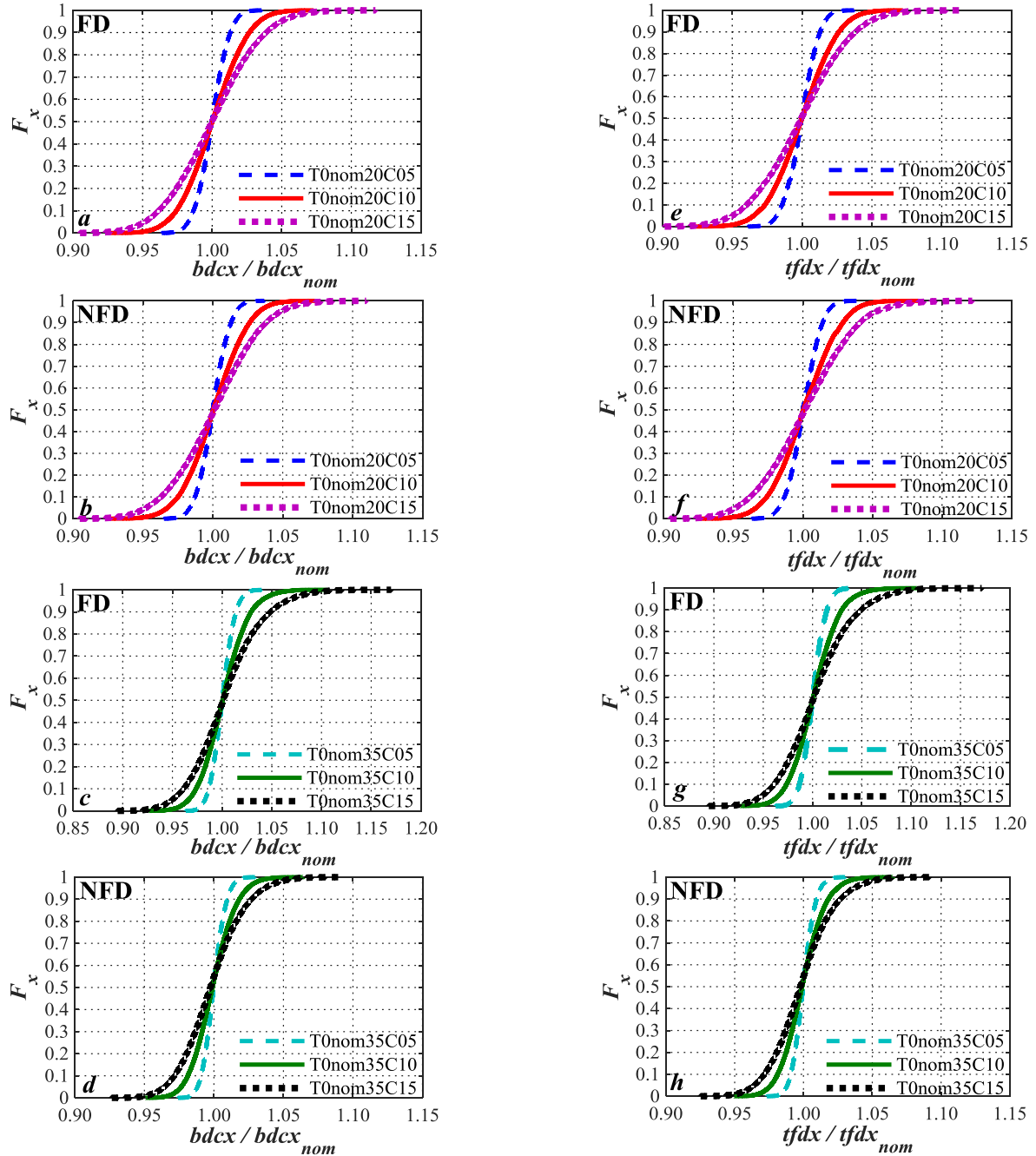
Fig. 9 Cumulative distribution function (CDF) plots for ((a) − (d)) normalized peak base displacement   and ((e) − (h)) normalized peak top floor displacement − calculated at the center of mass,   normalized with respect to corresponding nominal values, and averaged over all earthquakes

earthquakes vary in the ranges of 0.950~1.048, 0.902~1.106, and 0.856~1.171 for *C.O.V.* = 5%, 10%, and 15%, respectively. (2) There exists (i) no significant difference between the extreme values of a particular normalized structural response parameter and (ii) no specific increase/decrease trend, based on differences in earthquake type (FD and NFD) and isolation system period (2.0 s and 3.5 s). (3) Average normalized values of peak base displacements (*bdcx/bdcx$_{nom}$*) vary in the range of 0.963~1.047, 0.926~1.105, and 0.895~1.170 for *C.O.V.* = 5%, 10%, and 15%, respectively. (4) Average normalized

values of peak top floor displacements (*tfdx/tfdx$_{nom}$*) vary in the range of 0.961~1.047, 0.923~1.106, and 0.895~1.171 for *C.O.V.* = 5%, 10%, and 15%, respectively. (5) Average normalized values of peak top floor accelerations (*tfax/tfax$_{nom}$*) vary in the range of 0.950~1.048, 0.902~1.095, and 0.856~1.130 for *C.O.V.* = 5%, 10%, and 15%, respectively. (6) Average normalized values of peak base shear forces (*bsx/bsx$_{nom}$*) vary in the range of 0.952~1.044, 0.905~1.093, and 0.860~1.128 for *C.O.V.* = 5%, 10%, and 15%, respectively.
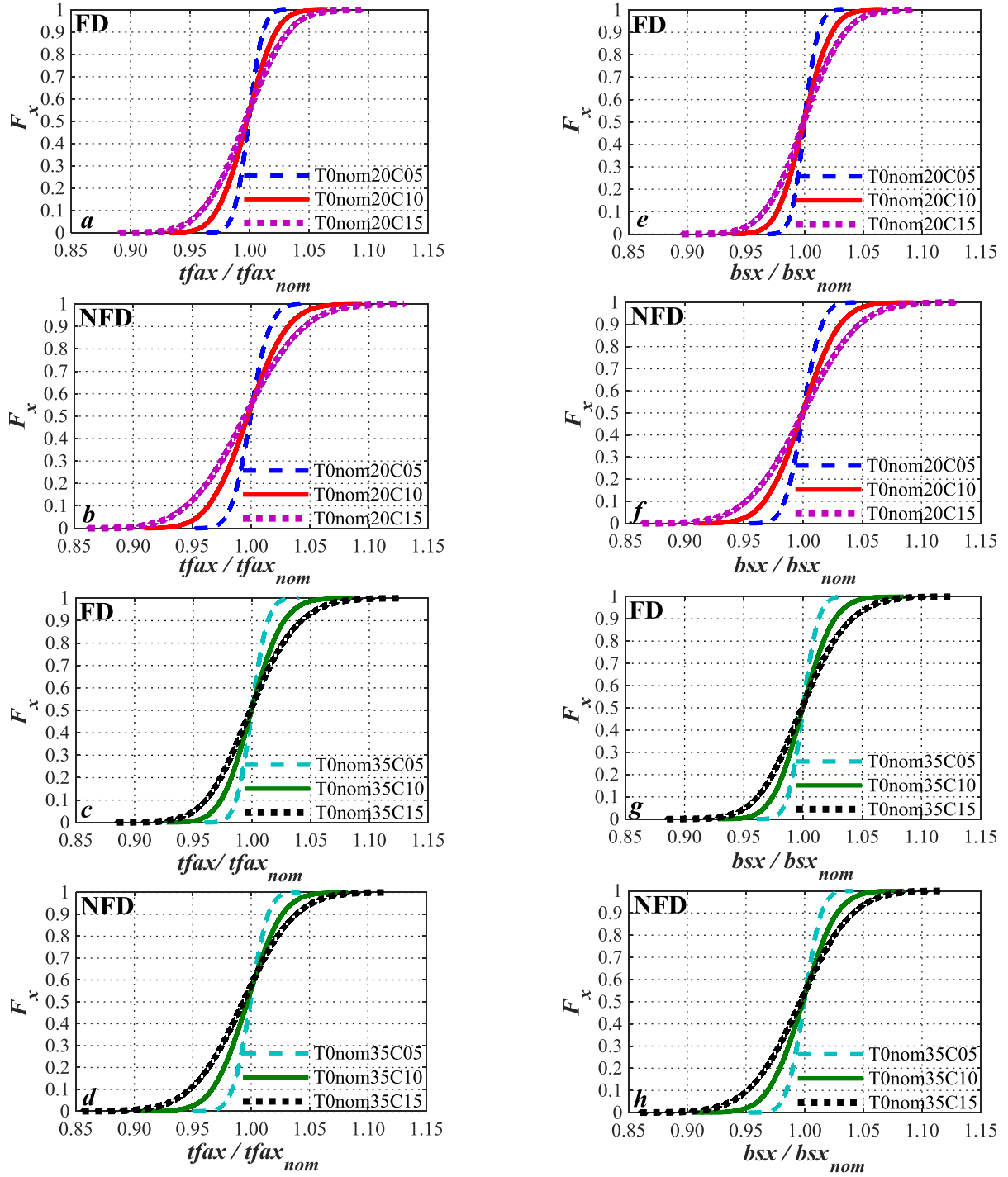
Fig. 10 Cumulative distribution function (CDF) plots for ((a) – (d)) peak top floor accelerations and ((e) – (h)) peak base shear forces − calculated at the center of mass, normalized with respect to corresponding nominal values, and averaged over all earthquakes

5.1 Percentile values

The pth percentile ($P_p/100$) of a variable is the value of that variable such that p percent of all the values of the subject variable are below that value while $(100-p)$ percent are above that value (Black 2009). That is, the pth percentile ($P_p/100$) of a variable (R) is equal to the value (R_j) of that

variable corresponding to $F_x(R_j) = p/100$ and calculated using Eq. (7).

$$F_x(R_j)=p/100 \rightarrow F_x^{-1}(p/100)=R_j=P_{p/100} \quad (7)$$

As a representative case for determination of the pth percentile using the CDF functions (i.e., F_x), the 90th percentile (i.e., $P_{0.90}$) of the normalized peak base
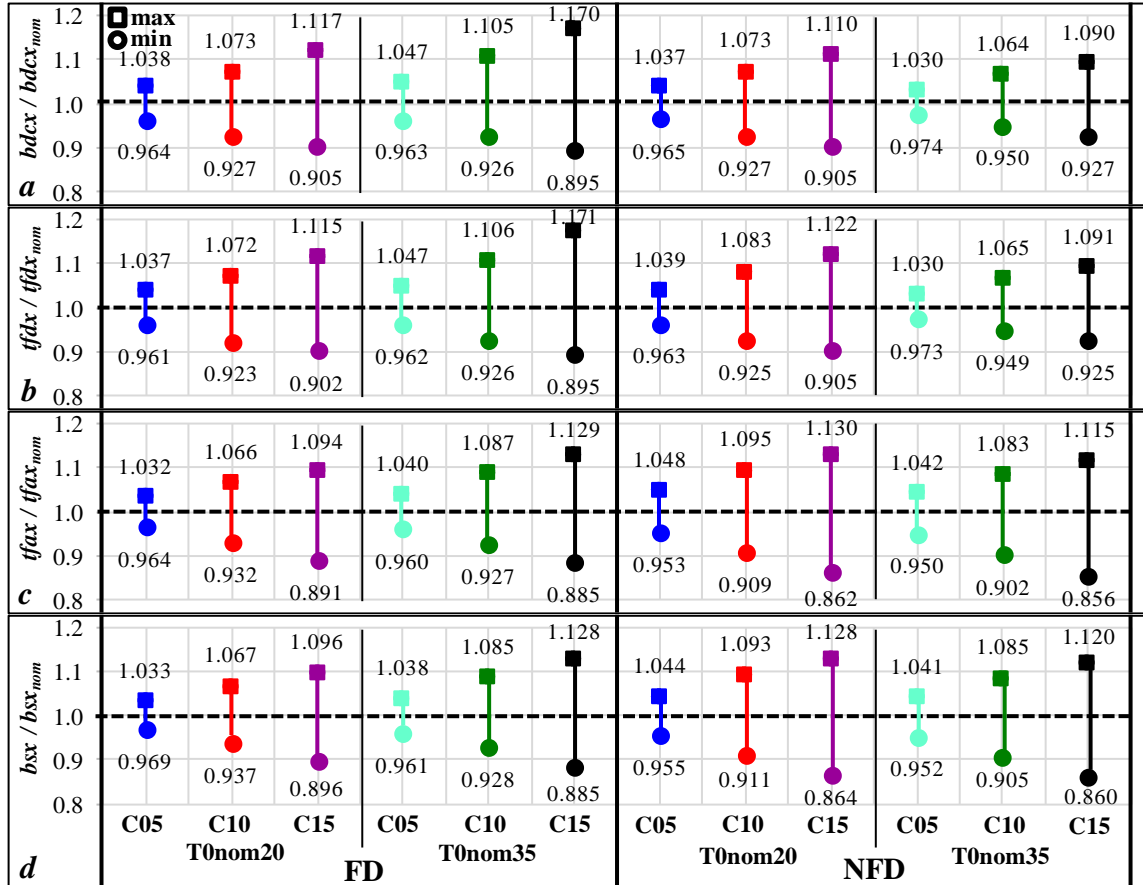
Fig. 11 The extreme values of the average normalized structural responses given in Figs. 9 and 10. The bold dashed line at 1.00 level represents the case where there is no deviation from the nominal response

displacement $bdcx/bdcx_{nom}$ is obtained as 1.05 corresponding to F_x = 0.90 in Fig. 12(a) for T0nom20C15 building subset subjected to the FD1 earthquake loading. The pth percentile of a variable can also be interpreted as the p percent safety level if that percentile value is considered as a limit state value. That is, there exists a 90% safety level (i.e., 10% of probability of exceedance) for T0nom20C15 building subset under FD1 if $bdcx/bdcx_{nom}$ =1.05 is considered as a limit state value.

The 80th ($P_{0.80}$), the 85th ($P_{0.85}$), the 90th ($P_{0.90}$), the 95th ($P_{0.95}$), and the 100th ($P_{1.00}$) percentiles of the percent deviations of the structural response parameters are evaluated in this chapter by making use of the CDF plots for each earthquake loading as demonstrated in Fig. 12(a). The absolute differences of the normalized peak structural responses from 1.00 gives us the percent deviations of a structural response parameter from its corresponding nominal value (please note that 1.00 level is shown with a bold dashed line in Fig. 11). For example, $bdcx/bdcx_{nom}$ = 1.05 stands for 5% deviation in peak base displacement response from its nominal value due to the uncertainties taken into account. The percentiles considered here (see Fig. 12(b)) allows us to portray the situation for different levels of safety (i.e., 80%, 85%, 90%, 95%, and 100%). In the representative plot given in Fig. 12(b), the percentile values of the percent deviations for T0nom20C15 building subset are given for all 27 FD loadings (shown with lines

with circular markers) along with the mean±one standard deviation values for peak base displacement. The percentiles of the deviation percentages of all structural response parameters are calculated for each of the six building subsets under each of the 27 FD loadings and the 27 NFD loadings, separately. The mean+one standard deviation values (for each percentile) calculated for $bdcx$, $tfdx$, $tfax$, and bsx obtained for each building subset are presented in Figs. 13(a), 14(a), 15(a), and 16(a), respectively. These figures are valuable as they demonstrate the results for each particular case and loading type. However, they also show that there exists no specific increase/decrease trend in deviation percentages of a particular structural response parameter at a particular p% safety level, based on differences in earthquake type (FD and NFD) or isolation system period (2.0 s and 3.5 s) whereas there exists a strong dependency on *C.O.V.* values. Consequently, in order to concentrate on the influence of the level of uncertainty (i.e., different *C.O.V.* values) at different p% safety levels, the averages of the mean+one standard deviation values of the percent deviations are calculated regardless of the earthquake type and the isolation period and given in Figs. 13(b), 14(b), 15(b), and 16(b), for $bdcx$, $tfdx$, $tfax$, and bsx, respectively. The general observations from Figs. 13(b), 14(b), 15(b), and 16(b), can be listed as follows: (1) Average mean+one standard deviation values of the percent deviations calculated for the
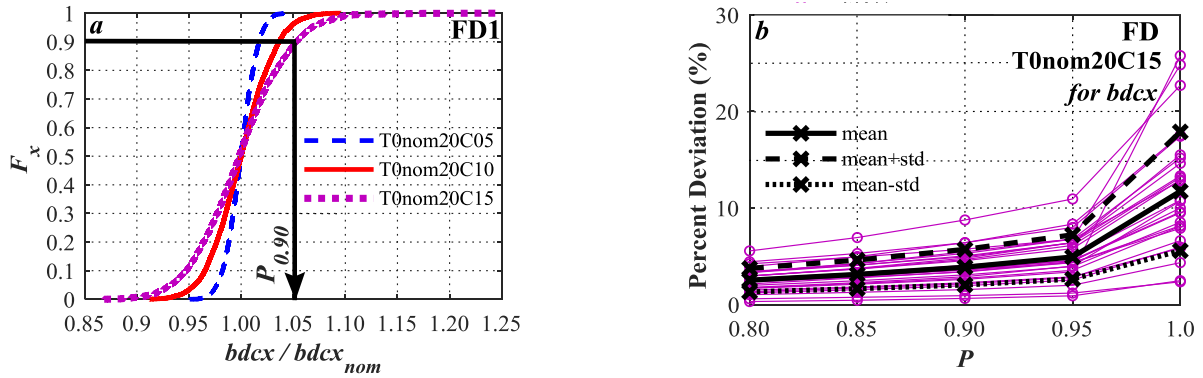
Fig. 12 (a) Sample percentile reading (90th percentile, i.e., $P_{0.90}$) from CDF plots (b) Percentile values of the percent deviations for T0nom20C15 building subset under FD loadings
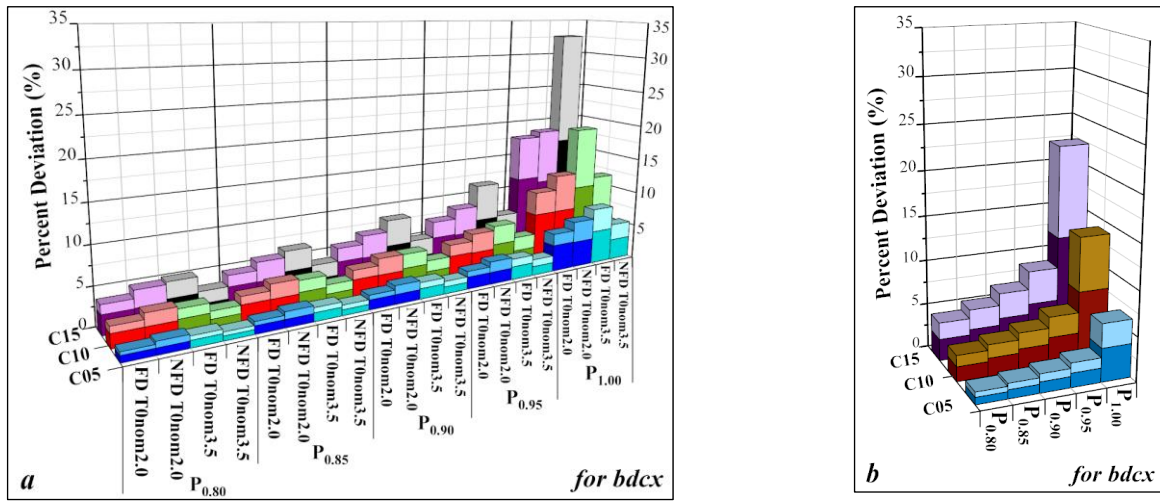

Fig. 13 Deviation percentages of peak base displacements for different percentiles. (a) for each isolation system period and earthquake loading type and (b) average values regardless of the earthquake type and the isolation period. [upper light colored portions of the columns represent the standard deviation and the lower dark colored portions stand for the mean values]
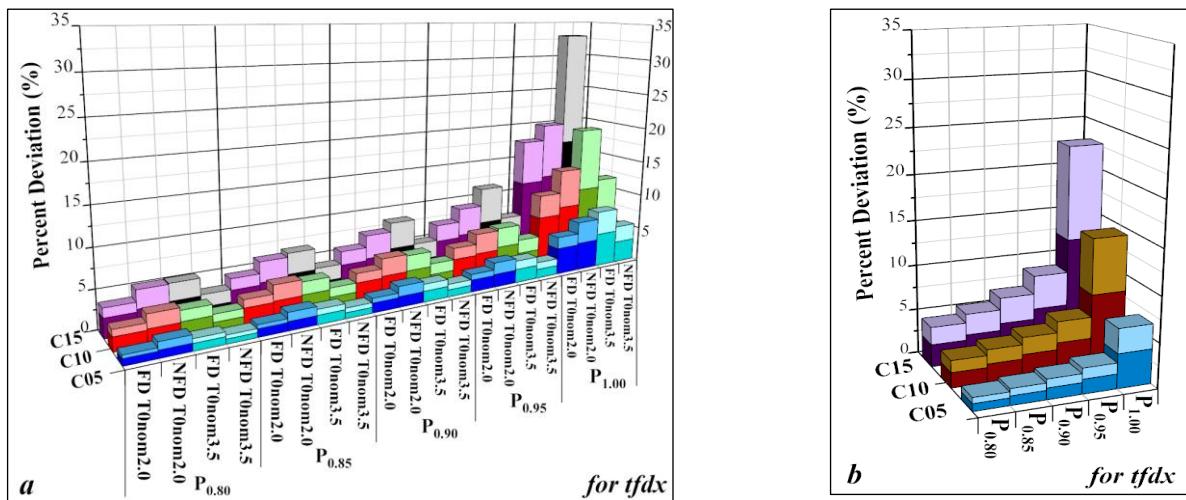

Fig. 14 Deviation percentages of peak top floor displacements for different percentiles. (a) for each isolation system period and earthquake loading type and (b) average values regardless of the earthquake type and the isolation period. [upper light colored portions of the columns represent the standard deviation and the lower dark colored portions stand for the mean values]
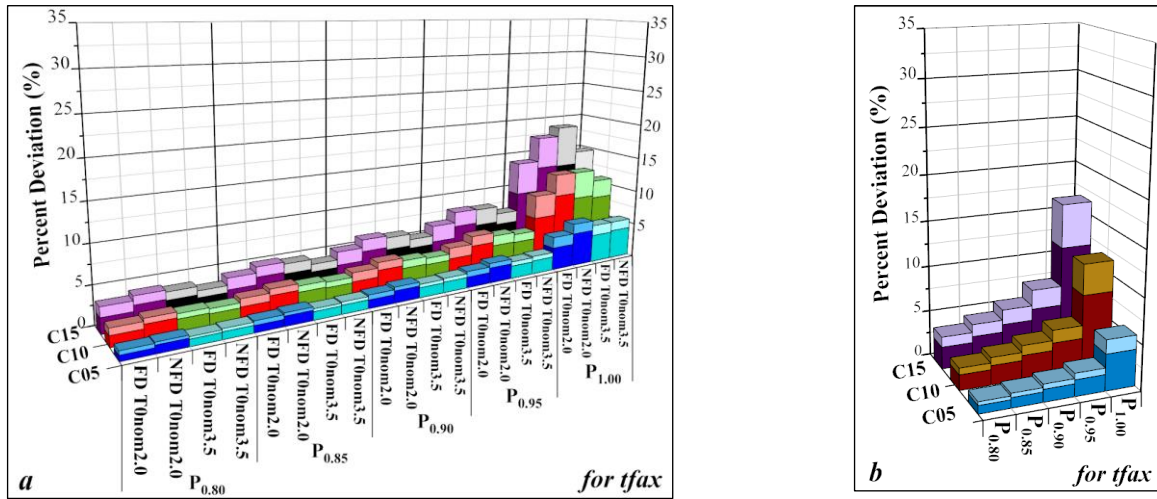
Fig. 15 Deviation percentages of peak top floor accelerations for different percentiles. (a) for each isolation system period and earthquake loading type and (b) average values regardless of the earthquake type and the isolation period. [upper light colored portions of the columns represent the standard deviation and the lower dark colored portions stand for the mean values]
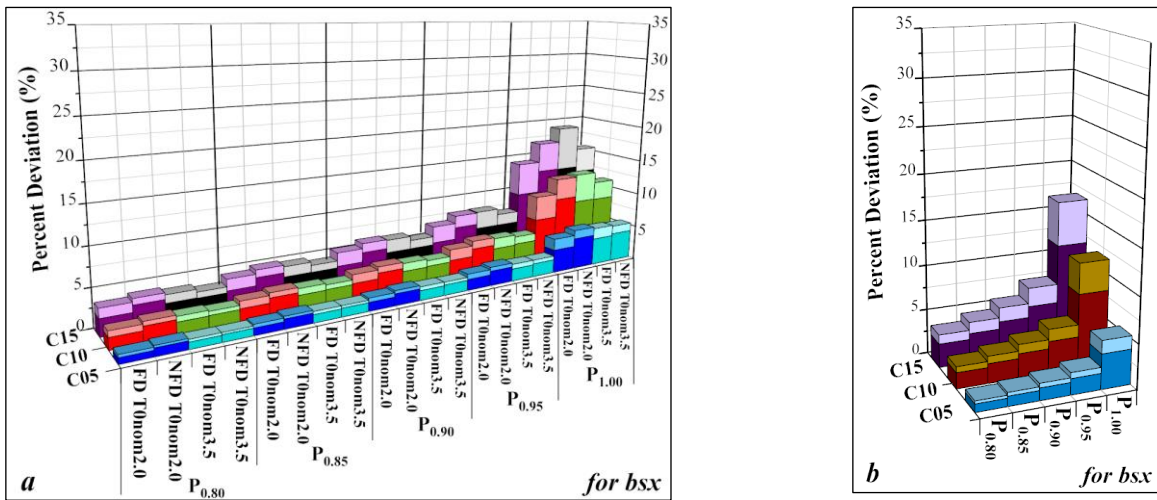

Fig. 16 Deviation percentages of peak base shear forces for different percentiles. (a) for each isolation system period and earthquake loading type and (b) average values regardless of the earthquake type and the isolation period. [upper light colored portions of the columns represent the standard deviation and the lower dark colored portions stand for the mean values]

displacement related parameters (*bdcx* and *tfdx*) - for a particular *C.O.V.* value- are considerably close to each other at the same p% safety levels. The same is true for acceleration related parameters (*tfax* and *bsx*). (2) Average mean+one standard deviation values of the percent deviations calculated for all response parameters increase gradually from the 80%, to the 85%, the 90%, and the 95% safety levels. (3) However, there are sudden jumps from the 95% to the 100% safety levels. (4) Both the amount of deviation and the deviation increments between all abovementioned safety levels increase as the *C.O.V.* values increase from 5% to 10%, and 15%.

For the 80% ~ 95% safety levels, average mean+one standard deviation values of the percent deviations calculated for *C.O.V.* = 5%, 10%, and 15% vary in the range of (i) 1.38%~2.74%, 2.91%~5.58%, and 4.30%~8.74%, respectively for the peak base displacements (*bdcx*) - Fig. 13(b); (ii) 1.49%~2.86%, 3.02%~5.70%, and 4.45%~8.81%, respectively for the peak top floor displacements (*tfdx*) - Fig. 14(b); (iii) 1.30%~2.54%, 2.44%~4.95%, and 3.57%~7.37%, respectively for the peak top floor accelerations (*tfax*) - Fig. 15(b); (4) 1.23%~2.45%, 2.43%~4.90%, and 3.67%~7.47%, respectively for the peak base shear forces (*bsx*) - Fig. 16(b). Evidently, the average mean+one standard deviation values of the percent
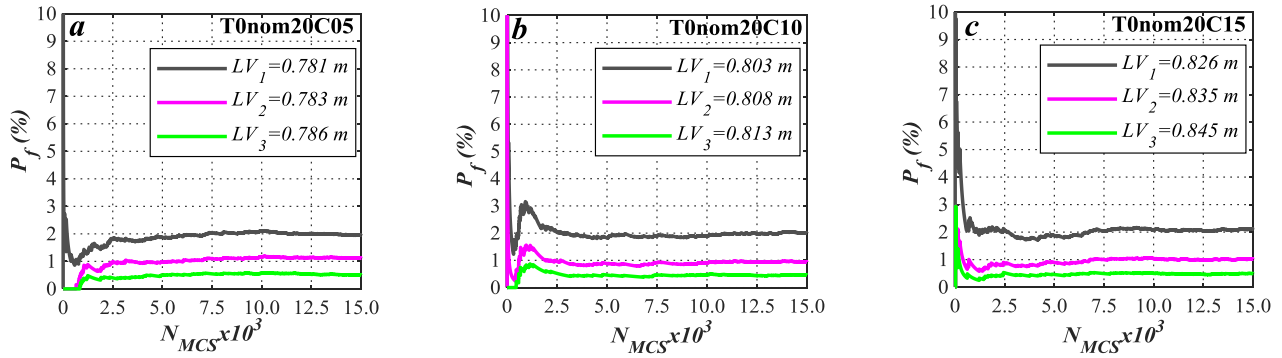
Fig. 17 Convergence of probability of failure for peak base displacements obtained under FD1 earthquake loading

deviations calculated for the 95% safety levels of all the response parameters are less than 3%, 6%, and 9% for *C.O.V.* = 5%, 10%, and 15%, respectively. That is, for the 95% safety level which may be considered as an acceptable reliability level for practical applications, a *C.O.V.* of 10% for isolator characteristics would be an acceptable target uncertainty level. Moreover, as long as a low (5%) or moderate (10%) *C.O.V.* value is targeted, the average mean+one standard deviation values of the percent deviations- even for the 100% safety- seems to be at an acceptable level. For *C.O.V.* = 5%, 10%, and 15%, they are calculated as (i) 6.49%, 13.97%, and 22.40%, respectively for the peak base displacements (*bdcx*) - Fig. 13(b); (ii) 6.59%,14.33%, and 22.80%, respectively for the peak top floor displacements (*tfdx*), Fig. 14(b); (iii) 5.58%, 11.69%, and 16.50%, respectively for the peak top floor accelerations (*tfax*) - Fig. 15(b); (4) 5.36%, 11.69%, and 16.64%, respectively for the peak base shear forces (*bsx*) - Fig. 16(b).

It should be noted that although not presented here due to space limitation, the results obtained for y-direction yields similar tendencies as the ones reported above for x-direction.

5.2 Verification of the adequacy number of Monte Carlo simulations

The accuracy and the efficiency of the Monte Carlo Simulation Method in probability investigations depend on the number of simulation cycles (Haldar and Mahadevan 2000). Therefore, before starting the Monte Carlo simulations, the appropriate number of the simulation cycles (N_{MCS}) to be realized is determined via a prior simulation study. In this prior simulation study, N_{MCS} is considered as 15000 at first and three different limit state values (*LV*) which would correspond to the probability of failures of 2.0%, 1.0%, and 0.5% are calculated. These values are LV_1=0.781 m, LV_2=0.783 m, and LV_3=0.786 m for T0nom20C05; LV_1=0.803 m, LV_2=0.808 m, and LV_3=0.813 m for T0nom20C10; and LV_1=0.826 m, LV_2=0.835 m, and LV_3=0.845 m for T0nom20C15 in terms of peak base displacement under FD1 earthquake loading, which is selected as a representative case presented here (see Fig. 17). Then, using these limit state values, it was checked whether these P_f values could be obtained

accurately with smaller number of simulation cycles.

The plots shown in Fig. 17 depict the variation of the probability of failures with respect to different number of simulation cycles for three different limit state values. As seen, the probability of failures corresponding to LV_1, LV_2, and LV_3 converge to P_f =2.0%, 1.0%, and 0.5%, respectively as N_{MCS} increases. Specifically, the convergence is successfully obtained for N_{MCS} over 5000, i.e. the tested probability of failure levels do not vary significantly for N_{MCS}>5000. Therefore, N_{MCS}=5000 is considered to be adequate for each of the 6 building subsets. That is, a total of 30.000 Monte Carlo simulations were conducted under each of the earthquake record pair and therefore, a total of 1.620.000 bidirectional nonlinear time history analyses were conducted for 6 building subsets under 54 earthquake record pairs.

6. Conclusions

In this study, the sensitivity of the probability of failures of the structures equipped with nonlinear isolation systems to the uncertainties in the isolator properties are investigated in terms of base displacement which is an isolation system response parameter and superstructure response parameters including top floor displacement and top floor acceleration, and base shear. A realistic three-dimensional multi-story building model was used in the framework of Monte Carlo Simulations. The inherent record-to-record variability nature of the earthquake ground motions is taken into account by carrying out analyses for a large number of ground motion records (a total of 54 pairs) which are classified as those with forward-directivity effects (FD) and without forward-directivity effects (NFD). In order to consider the uncertainties in the isolation system characteristics, the pre-yield stiffness, post-yield stiffness, and yield displacement characteristics of each isolator are assumed as random variables. Two different levels of nominal isolation periods representing long and short isolation system periods (T_0=2.0 s and 3.5 s) -each with three different levels of uncertainty (coefficient of variation (*C.O.V.*) = 5% to 10%, and 15%)- are considered. Following conclusions are reached:

• It is determined that the uncertainty that exists in the isolator characteristics affect the structural response

which steadily increase as the coefficient of variation (*C.O.V.*) increases.

• The shapes of CDF plots of the peak base displacements and the peak top floor displacements -for a particular building subset and earthquake loading- in general resemble each other. The same is true for the peak top floor accelerations and the peak base shear forces.

• The probabilistic sensitivity of a base-isolated building does not show a particular trend based on the earthquake loading type (FD or NFD) or isolation system period (long or short).

• The extreme values of the normalized structural responses (average of all cases) –which represent deviations from the nominal responses- corresponding to the highest and the lowest probability of exceedance vary in the ranges of 0.95~1.05, 0.90~1.11, and 0.86~1.17 for *C.O.V.*=5%, 10%, and 15%, respectively.

• The average mean+one standard deviation values of the percent deviations are calculated for all structural response parameters which increase gradually from the 80% to the 95% safety level with sudden jumps observed for a switch from the 95% to the 100% safety level.

• Average mean+one standard deviation values of the percent deviations calculated for the 95% safety levels of all the response parameters are less than 3%, 6%, and 9% for the cases, whose *C.O.V.* values are equal to 5%, 10%, and 15%, respectively. Evidently, for a 95% safety, which may be considered as an acceptable reliability level for practical applications, a *C.O.V.* of 10% for isolator characteristics would be an acceptable target uncertainty level.

• Comparative plots of cumulative distribution functions presented for different uncertainty levels (*C.O.V.* = 5% to 10%, and 15%) and related statistical evaluation portray the potential extent of the deviation of the structural response parameters, which is expected to be useful for practicing engineers in evaluating isolator test results for their projects.

• Cumulative distribution plots presented in this study provide a comprehensive information which can be used in determining probability of failure values corresponding to various selected limit states relating to rupture and/or buckling of isolators and partial or complete collapse of the structural system, or breakdown of sensitive machinery equipment.

Acknowledgments

References

Alhan, C. and Gavin, H.P. (2004), "A parametric study of linear and non-linear passively damped seismic isolation systems for buildings", *Eng. Struct.*, **26**(4), 485-497.

Alhan, C. and Gavin, H.P. (2005), "Reliability of base isolation for the protection of critical equipment from earthquake hazards", *Eng. Struct.*, **27**, 1435-1449.

Alhan, C. and Gazi, H. (2014), "Bringing probabilistic analysis perspective into structural engineering education: use of monte carlo simulations", *Int. J. Eng. Educ.*, **30**(5), 280-1294.

Alhan, C. and Hışman, K. (2016), "Seismic isolation performance sensitivity to potential deviations from design values", *Smart Struct. Syst.*, **18**(2), 293-315.

Alhan, C., Gazi, H. and Kurtuluş, H. (2016), "Significance of stiffening of high damping rubber bearings on the response of base-isolated buildings under near-fault earthquakes", *Mech. Syst. Signal Pr.*, **79**, 297-313.

ASCE/SEI 7-10 (2010), *Minimum Design Loads for Buildings and Other Structures*, American Society of Civil Engineers, Structural Engineering Institute, Virginia, USA.

Black, K. (2009), *Business Statistics for Contemporary Decision Making*, (6th Ed.), John Wiley and Sons Inc., USA.

Bray, J.D. and Marek, A.R. (2004), "Characterization of forward-directivity ground motions in the near-fault region", *Soil Dyn. Earthq. Eng.*, **24**, 815-828.

Castaldo, P., Amendola, G. and Palazzo, B. (2017), "Seismic fragility and reliability of structures isolated by friction pendulum devices: seismic reliability based design (SRBD)", *Earthq. Eng. Struct. D.*, **46**(3), 425-446.

Cheng, F.Y., Jiang, H. and Lou, K. (2008), *Smart Structures Innovative Systems for Seismic Response Control*, CRC Press Taylor & Francis Group, Boca Raton, Florida, USA.

Choun, Y.S., Park, J. and Choi, I.K. (2014), "Effects of mechanical property variability in lead rubber bearings on the response of seismic isolation system for different ground motions", *Nucl. Eng. Technol.*, **46**(5), 605-618.

Constantinou, M.C., Tsopelas, P., Kasalanati, A. and Wolf, E.D. (1999), *Property Modification Factors for Seismic Isolation Bearings (Technical Report MCEER-99-0012)*, University at Buffalo, New York, USA.

Datta, T.K. (2010), *Seismic Analysis of Structures*, John Wiley & Sons (Asia) Pte Ltd, Singapore.

De La Llera, J.C. and Inaudi, J.A. (1994), "Analysis of base-isolated buildings considering stiffness uncertainty in the isolation system", *Proceedings of the 5th U.S. National Conference on Earthquake Engineering*, Chicago, Illinois, USA, July.

Dicleli, M. and Buddaram, S. (2007), "Equivalent linear analysis of seismic-isolated bridges subjected to near-fault ground motions with forward rupture directivity effect", *Eng. Struct.*, **29**, 21-32.

DIS (2007), *Seismic Isolation for Buildings and Bridges*, Dynamic Isolation Systems, McCarran, Nevada, USA.

Fan, F.G., Ahmadi, G., Mostaghel, N. and Tadjbakhsh, I.G. (1991), "Performance analysis of aseismic base isolation systems for a multi-story building", *Soil Dyn. Earthq. Eng.*, **10**(3), 152-171.

Fan, J. and Zhang, Y. (2014), "A hybrid probability-convex model for the seismic demand analysis of bearing displacement in the benchmark base-isolated structure", *Adv. Struct. Eng.*, **17**(7), 1061-1073.

Gazi, H. (2015), "Probabilistic behavior of seismically isolated buildings under earthquake loadings" PhD dissertation, İstanbul University, İstanbul, Turkey.

Haldar, A. and Mahadevan, S. (2000), *Probability Reliability and Statistical Methods in Engineering Design*, John Wiley & Sons Inc., USA.

Han, R., Li, Y. and Lindt, J. (2014), "Seismic risk of base isolated non-ductile reinforced concrete buildings considering uncertainties and mainshock-aftershock sequences", *Struct. Saf.*, **50**, 39-56.

Hirata, K., Shiojiri, H., Mazda, T. and Kontani, O. (1989), "Response variability of isolated structure due to randomness of isolation devices", *ICOSSAR 89 Proceedings of the 5th International Conference on Structural Safety and Reliability*, San Francisco, California, USA, August.

Jacob, C., Sepahvand, K., Matsagar, V.A. and Marburg, S. (2013), "Stochastic seismic response of base-isolated buildings", *Int. J. Appl. Mech.*, **5**(1), 1350006 (21 pages).

Jangid, R.S. (2010), "Stochastic response of building frames isolated by lead-rubber bearings", *Struct. Control Health.*, **17**(1), 1–22.

Jangid, R.S. and Datta, T.K. (1995a), "The stochastic response of asymmetric base isolated buildings", *J. Sound Vib.*, **179**(3), 463-473.

Jangid, R.S. and Datta, T.K. (1995b), "Performance of base-isolation systems for asymmetric building subject to random-excitation", *Eng. Struct.*, **17**(6), 443-454.

Kelly, T.E. (2001), *Base Isolation of Structures*, Holmes Consulting Group Ltd., Wellington, New Zealand.

Kilar, V. and Koren, D. (2009), "Seismic behavior of asymmetric base isolated structures with various distributions of isolators", *Eng. Struct.*, **31**, 910-921.

Kumar, M. (2015), "Seismic isolation of nuclear power plants using elastomeric bearings", PhD dissertation, University at Buffalo, State University of New York, New York, USA.

Ma, C., Zhang, Y., Zhao, Y., Tan, P. and Zhou, F. (2011), "Stochastic seismic response analysis of base-isolated high-rise buildings", *Procedia Engineer.*, **14**, 2468–2474.

Ma, C.F., Zhang, Y.H., Tan P. and Zhou, F.L. (2014), "Seismic response of base-isolated high-rise buildings under fully nonstationary excitation", *Shock and Vib.*, **2014**, 401469 (Article id), 11 pages.

Malhotra, P.K. (1999), "Response of buildings to near-field pulse-like ground motions", *Earthq. Eng. Struct. D.*, **28**, 1309-1326.

Marano, G.C. and Greco, R. (2003), "Efficiency of base isolation systems in structural seismic protection and energetic assessment", *Earthq. Eng. Struct. D.*, **32**, 1505-1531.

Mathworks (2009), *MATLAB: The Language of Technical Computing, Version 7.8.0 (R2009a)*, The Math Works Inc., USA.

Matsagar, V.A. and Jangid, R.S. (2005), "Base-isolated building with asymmetries due to the isolator parameters", *Adv. Struct. Eng.*, **8**, 603-621.

Mazza, F. Vulcano, A. and Mazza, M. (2012), "Nonlinear dynamic response of RC buildings with different base isolation systems subjected to horizontal and vertical components of near-fault ground motions", *The Open Construction & Building Technology Journal*, **6**, 373-383.

Mishra, S.K. and Chakraborty, S. (2013), "Performance of a base-isolated building with system parameter uncertainty subjected to a stochastic earthquake", *Int. J. Acoust. Vib.*, **18**(1), 7-19.

Naeim, F. and Kelly, J.M. (1999), *Design of Seismic Isolated Structures from Theory to Practice*, Wiley, New York, USA.

Nagarajaiah, S., Reinhorn, A.M. and Constantinou, M.C. (1991), *3D-BASIS: A General Program for the Nonlinear Dynamic Analysis of three Dimensional Base Isolated Buildings*, National Center for Earthquake Engineering Research, State University of New York at Buffalo, New York, USA.

Okamura, S. and Fujita, S. (2007), "Motion analysis of pendulum type isolation systems during earthquakes (probabilistic study of isolation performance of base isolated structure considering characteristic dispersion of pendulum type isolation systems)", *J. Press. Vess-T. ASME*, **129**(3), 507-515.

PEER (2011), Pacific Earthquake Engineering Resource Center: NGA Database, http://ngawest2.berkeley.edu/

Pinto, P.E. and Vanzi, I. (1992), "Base-isolation: reliability for different design criteria", *Proceedings of the Earthquake Engineering Tenth World Conference*, Madrid, Spain, July.

Politopoulos, I. and Pham, H.K., (2009), "Sensitivity of seismically isolated structures", *Earthq. Eng. Struct. D.*, **38**, 989–1007.

Politopoulos, I. and Sollogoub, P. (2005), "Vulnerability of elastomeric bearing isolated buildings and their equipment", *J. Earthq. Eng.*, **9**(4), 525-546.

Providakis, C.P. (2009), "Effect of supplemental damping on LRB and FPS seismic isolators under near-fault ground motion", *Soil Dyn. Earthq. Eng.*, **29**, 80-90.

Ryan, K.L. and Chopra, A.K. (2004), "Estimation of Seismic Demands on Isolators Based on Nonlinear Analysis, *J. Struct. Eng.*, **130**(3), 392-402.

Ryan, K.L. and Earl, C.L. (2010), "Analysis and design of inter-story isolation systems with nonlinear devices", *J. Earthq. Eng*, **14**, 1044-1062.

Sehhati, R., Rodriguez-Marek, A., Elgawady, M. and Cofer, W.F. (2011), "Effect of near-fault ground motions and equivalent pulses on multi-story structures", *Eng. Struct.*, **33**, 767-779.

Sharma, A. and Jangid, R.S. (2009), "Behavior of Base-Isolated Structures with High Initial Isolator Stiffness", *Int. J. Civil Environ. Struct. Constr. Architect. Eng.*, **3**(2), 49-54.

Shenton III, H.W. and Holloway, E.S. (2000), "Effect of stiffness variability on the response of isolated structures", *Earthq. Eng. Struct. D.*, **29**, 19-36.

Somerville, P. (2005), "Engineering characterization of near fault ground motions", *Planning and Engineering for Performance in Earthquakes (2005 NZSEE)*, New Zealand, March.

Su, L., Ahmadi, G. and Tadjbakhsh, I. (1990a), "A comparative study of performances of various base isolation systems part II: sensitivity analysis", *Earthq. Eng. Struct. D.*, **19**, 21-33.

Tena-Colunga, A. and Escamilla-Cruz, J.L. (2007), "Torsional amplifications in asymmetric base-isolated structures", *Eng. Struct.*, **29**, 237-247.

Tena-Colunga, A. and Zambrana-Rojas, C. (2006), "Dynamic torsional amplifications of base-isolated structures with an eccentric isolation system", *Eng. Struct.*, **28**, 72–83.

Yoo, B. and Kim, Y.H. (2002), "Study on effects of damping in laminated rubber bearings on seismic responses for a ⅛ scale isolated test structure", *Earthq. Eng. Struct. D.*, **31**(10), 1777-1792.

FC